[16] G. Barbiellini and S. Orito, in *Proceedings of the European Physical Society International Conference on Meson Resonances and Related Electromagnetic Phenomena, Bologna, Italy, 1971,* edited by R. H. Dalitz and A. Zichichi (Editrice Compositori, Bologna, Italy, 1972), p. 505.

[17] The author thanks S. Orito for giving him this crucial information.

[18] R. J. Crewther, Phys. Rev. Lett. 28, 1421 (1972).

[19] M. S. Chanowitz and J. Ellis, Phys. Lett. 40B, 397 (1972); Phys. Rev. D 7, 2490 (1973).

[20] G. Mack, Nucl. Phys. B5, 499 (1968). The PCDC anomaly was found by Coleman and Jackiw in the Callan-Symanzik equation for currents. See S. Coleman and R. Jackiw, Ann. Phys. (N.Y.) 67, 552 (1971).

[21] The Callan-Symanzik anomaly is assumed to be absent [C. G. Callan, Phys. Rev. D 2, 1541 (1970); K. Symanzik, Commun. Math. Phys. 18, 227 (1970)].

[22] R. J. Crewther, Phys. Lett. 33B, 305 (1970).

[23] J. Ellis, Nucl. Phys. B22, 478 (1970).

[24] Notice that in (11) the errors due to the extrapolation needed from $m_\epsilon^2 = 0$ to $m_\epsilon^2 = (700\text{ MeV})^2$ would best be compensated by each other.

[25] To determine $f_V^2/4\pi$, we have used the formula

$$\Gamma_{V\to l^+l^-} = (e^4/12\pi f_V^2) m_V (1 + 2m_l^2/m_V^2)(1 - 4m_l^2/m_V^2)^{1/2}$$

for the decay width of the vector meson V into a lepton pair l^+l^-, and the present particle data,

$$\Gamma_{\rho\to e^+e^-} = (146 \pm 10)(0.0043 \pm 0.0005) \times 10^{-2}\text{ MeV},$$

$$\Gamma_{\omega\to e^+e^-} = (9.8 \pm 0.5)(0.0076 \pm 0.0017) \times 10^{-2}\text{ MeV},$$

and

$$\Gamma_{\phi\to e^+e^-} = (4.2 \pm 0.2)(0.032 \pm 0.003) \times 10^{-2}\text{ MeV}.$$

See Particle Data Group, Rev. Mod. Phys. 45, S1 (1973).

[26] S. Orito has informed me that the invariant masses of π^+ and π^- found in the two candidates for $e^+ + e^- \to e^+ + e^- + \pi^+ + \pi^-$ are about 700 MeV ($\cong m_\epsilon$) and 1300 MeV ($\cong m_f$). Subtracting the Born contribution (~2.0 nb) as background from the Frascati data (σ ~3.3 nb), we find that a *very rough estimate* of R is about 6.5. Very lately, Orito *et al.* have made a more detailed analysis of their data including an additional candidate for $\gamma + \gamma \to \epsilon$ in the same way as discussed in this paper, concluding $R = 5.8^{+3.2}_{-3.5}$. See S. Orito, M. L. Ferrer, L. Paoluzi, and R. Santonico, Phys. Lett. 48B, 380 (1974).

[27] A. Bramón, E. Etim, and M. Greco, Phys. Lett. 41B, 609 (1972).

[28] J. J. Sakurai, Phys. Lett. 46B, 207 (1973).

[29] This point has come out of the discussion with P. Langacker.

[30] J. Pestieau and J. Terazawa, Phys. Rev. Lett. 24, 1149 (1970).

[31] A. I. Sanda, Phys. Rev. D (to be published).

[32] S. M. Berman, J. D. Bjorken, and J. B. Kogut, Phys. Rev. D 4, 3388 (1971).

[33] A. Pais and S. B. Treiman, Phys. Rev. Lett. 25, 975 (1970).

PHYSICAL REVIEW D VOLUME 9, NUMBER 5 1 MARCH 1974

Analysis for hypercharge-exchange reactions in terms of dispersion relations

E. N. Argyres*
State University College of Arts and Science, Plattsburgh, New York 12901

A. P. Contogouris†‡
Brookhaven National Laboratory, Upton, New York 11973

J. P. Holden§
McGill University, Montreal, Quebec, Canada

(Received 16 July 1973)

An analysis of $\pi N \to K\Lambda$ and $\bar{K}N \to \pi\Lambda$ is presented in which the imaginary parts of the amplitudes are in approximate agreement with finite-energy sum rules and the real parts are calculated in terms of the imaginary parts via fixed-t dispersion relations. The resulting differential cross sections and polarizations are in fair agreement with experiment. Certain features and implications of the amplitude structure are discussed.

I. INTRODUCTION

Line-reversed hypercharge-exchange reactions present a number of intriguing features which cannot be understood in terms of simple Regge phenomenology. For example, it has been known for quite some time[1] that a model with a pair of exchange-degenerate Regge poles K^*-K^{**} is in clear contradiction with basic experimental facts. One may hope that amplitude analysis, which has thrown much light on the structure of πN amplitudes, will provide some insight into the problems of hypercharge exchange as well. One may also hope that through such an analysis a common picture of the structure of amplitudes of nondiffractive two-body reactions will eventually emerge.

Recently amplitude analyses of hypercharge-exchange reactions have been published by Barger and Martin[2] and by Irving, Martin, and Barger.[3] Unlike πN scattering, these analyses are not completely model-independent; certain assumptions motivated by the results of the $\pi^- p \to \pi^0 n$ analyses are necessary. The resulting amplitudes, however, exhibit a number of interesting features and provide very useful information.

The purpose of the present work is to present a set of amplitudes for $\pi N \to K\Lambda$ and $\bar{K}N \to \pi\Lambda$ in which (a) the imaginary parts of the amplitudes are in approximate agreement with finite-energy sum rules (FESR), (b) the real parts of the amplitudes are calculated in terms of the above imaginary parts by means of fixed-t dispersion relations, and (c) the resulting amplitudes give differential cross sections and polarizations in fair agreement with experiment.

The starting point of our work is a set of imaginary parts consistent with the analyses of Barger *et al.*[2,3] (to be subsequently denoted as the BMI solution). Then fixed-t dispersion relations, together with the available experimental information on the low-energy region of $\pi N \to K\Lambda$ and $\bar{K}N \to \pi\Lambda$, determine the real parts. This approach has been tested in detail in πN charge exchange,[4-6] in charged[7] and neutral[8] pion photoproduction, and to some extent in KN charge exchange[5,8]; it has also been applied in hypercharge-exchange reactions ("hybrid" model),[9] but in a somewhat different way.

Section II presents the essentials of the formalism to be used in our calculation. Section III discusses the details of our procedure, in particular in fixing the contributions (resonance parameters) of the low-energy region. Section IV discusses the basic features of our calculated real parts and compares them with those of Barger *et al.*,[2,3] as well as with the corresponding quantities (vector and tensor exchanges) of charge-exchange reactions; it also compares with experiment our differential cross sections and polarizations. Finally, Sec. V summarizes our conclusions and discusses certain possible implications.

II. GENERAL FORMALISM

In this section we outline the basic formalism used to describe the two line-reversed reactions shown in Fig. 1. The s channel is taken as $K^- n \to \pi^- \Lambda$ and is described by amplitudes $A(\nu, t)$ and $B(\nu, t)$, where $4M_N\nu = s-u$. The corresponding u-channel amplitudes describing $\pi^+ n \to K^+\Lambda$ are

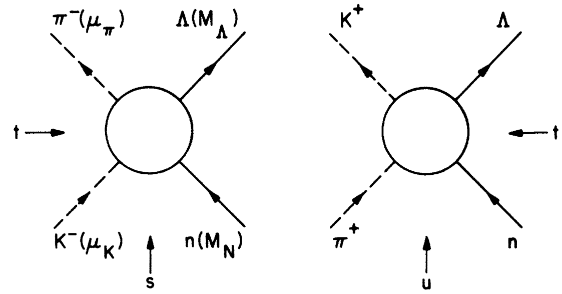

FIG. 1. Kinematics of the line-reversed reactions $K^- n \to \pi^- \Lambda$ and $\pi^+ n \to K^+ \Lambda$.

denoted by $\bar{A}(\nu, t)$ and $\bar{B}(\nu, t)$. Since our approach is based on dispersion relations, we need crossing-symmetric combinations of these amplitudes. These are conveniently taken as[9]

$$A^{(\pm)}(\nu, t) = \tfrac{1}{2}[A(\nu, t) \pm \bar{A}(\nu, t)]$$
$$= \tfrac{1}{2}[A(\nu, t) \pm A(-\nu, t)], \quad (1.1)$$

$$B^{(\pm)}(\nu, t) = \tfrac{1}{2}[B(\nu, t) \pm \bar{B}(\nu, t)],$$
$$= \tfrac{1}{2}[B(\nu, t) \mp B(-\nu, t)]; \quad (1.2)$$

for large ν these correspond to exchanges of definite signature in the t channel. The corresponding nonflip and flip s-channel helicity amplitudes (SHA) are, to leading order in ν,

$$F_0^{(\pm)}(\nu, t) = -2\bar{M}\left[A^{(\pm)}(\nu, t) + \frac{M_N}{\bar{M}}\nu B^{(\pm)}(\nu, t)\right], \quad (1.3)$$

$$F_1^{(\pm)}(\nu, t) = -\sqrt{-t}\, A^{(\pm)}(\nu, t), \quad (1.4)$$

with $2\bar{M} = M_N + M_\Lambda$. The amplitudes for $K^- n \to \pi^- \Lambda$ are then $F_n = F_n^{(+)} + F_n^{(-)}$, while those for $\pi^+ n \to K^+\Lambda$ take the form $\bar{F}_n = F_n^{(+)} - F_n^{(-)}$. Notice that with these sign conventions exchange degeneracy (EXD) would imply $\mathrm{Im}F_n^{(+)} = -\mathrm{Im}F_n^{(-)}$. The amplitudes are normalized so that

$$\frac{d\sigma}{dt} = \frac{1}{64\pi s p_s^{\,2}}(|F_0|^2 + |F_1|^2), \quad (1.5)$$

$$P\frac{d\sigma}{dt} = \frac{1}{32\pi s p_s^{\,2}}\,\mathrm{Im}(F_0 F_1^*) \quad (1.6)$$

in the s channel; analogous relations hold for the barred amplitudes.

The amplitudes $A^{(\pm)}$ and $B^{(\pm)}$ have definite crossing properties and are expected to satisfy the following dispersion relations, apart from possible subtractions (see below):

$$\mathrm{Re}A^{(\pm)}(\nu, t) = \frac{1}{\pi}\,\mathrm{P}\int_0^\infty dx\,\mathrm{Im}A^{(\pm)}(x, t)\left(\frac{1}{x-\nu} \pm \frac{1}{x+\nu}\right), \quad (1.7)$$

$$\mathrm{Re}B^{(\pm)}(\nu, t)=\frac{1}{\pi}\,\mathrm{P}\int_0^{\infty} dx\,\mathrm{Im}B^{(\pm)}(x, t)\left(\frac{1}{x-\nu}\mp\frac{1}{x+\nu}\right). \tag{1.8}$$

We assume that the asymptotic form of the imaginary parts of the amplitudes at large ν, say, $\nu>\nu_M$, can be represented by effective Regge-type contributions of the form

$$\mathrm{Im}A^{(\pm)}(\nu, t)\simeq a^{(\pm)}(t)\nu^{\alpha_{\pm}(t)}\ ,$$
$$\mathrm{Im}B^{(\pm)}(\nu, t)\simeq b^{(\pm)}(t)\nu^{\alpha'_{\pm}(t)-1}\ . \tag{1.9}$$

Here $\alpha_{\pm}(t)$ and $\alpha'_{\pm}(t)$ are effective Regge exponents. In this way the above expressions for $\mathrm{Im}A^{(-)}$ and $\mathrm{Im}B^{(-)}$ represent the over-all vector (K^*) exchange contributions (Regge-pole exchange plus absorption or other corrections). Similarly the expressions for $\mathrm{Im}A^{(+)}$ and $\mathrm{Im}B^{(+)}$ of (1.9) represent over-all tensor ($K^{**}\equiv Q$) exchange. It will be convenient to define

$$A^{(\pm)}_{\rm asy}(\nu, t)=\xi^{(\pm)}(t)a^{(\pm)}(t)\nu^{\alpha_{\pm}(t)},$$
$$B^{(\pm)}_{\rm asy}(\nu, t)=\xi'^{(\pm)}(t)b^{(\pm)}(t)\nu^{\alpha'_{\pm}(t)-1}, \tag{1.10}$$

where

$$\xi^{(\pm)}(t)=-\frac{\pm 1+e^{-i\pi\alpha_{\pm}(t)}}{\sin\pi\alpha_{\pm}(t)}\ . \tag{1.11}$$

Thus for $\nu>\nu_M$

$$\mathrm{Im}A^{(\pm)}(\nu, t)\simeq\mathrm{Im}A^{(\pm)}_{\rm asy}(\nu, t),$$
$$\mathrm{Im}B^{(\pm)}(\nu, t)\simeq\mathrm{Im}B^{(\pm)}_{\rm asy}(\nu, t)\,. \tag{1.12}$$

In general $\alpha'_{\pm}(t)$ need not be the same as $\alpha_{\pm}(t)$. However, for simplicity and in accord with Ref. 2 we take

$$\alpha_{\pm}(t)=\alpha'_{\pm}(t)\equiv\alpha(t)=0.4+t\ . \tag{1.13}$$

As in Refs. 4–9, we proceed by splitting the dispersion integrals of (1.7), (1.8) in two pieces: a low-energy piece, $0<\nu<\nu_M$, where $\mathrm{Im}A^{(\pm)}$ and $\mathrm{Im}B^{(\pm)}$ are calculated in terms of low-energy experimental information, and a high-energy piece, $\nu_M<\nu<\infty$, where we use the expressions (1.9) with (1.13). Numerous calculations, including those of Refs. 4–9, show that above $p_{\rm lab}\approx 3$ GeV/c such expressions provide good parametrizations of the imaginary parts of the amplitudes. Then the most reliable way to calculate real parts should be through dispersion relations (DR).

The DR for $A^{(+)}$ requires a subtraction; thus we shall write a DR for the difference $A^{(+)}-A^{(+)}_{\rm asy}$. The rest do not require subtractions; nevertheless, by splitting the dispersion integrals as above and using well-known Hilbert transforms (see e.g., the Appendix of Ref. 2), we can write all DR in the form

$$\mathrm{Re}A^{(\pm)}(\nu, t)=\mathrm{Re}A^{(\pm)}_{\rm asy}(\nu, t)+\frac{1}{\pi}\int_0^{\nu_M} dx\,\mathrm{Im}\,A^{(\pm)}(x, t)\left(\frac{1}{x-\nu}\pm\frac{1}{x-\nu}\right)-a^{(\pm)}(t)S^{(\pm)}(\nu, t), \tag{1.14}$$

$$\mathrm{Re}B^{(\pm)}(\nu, t)=\mathrm{Re}B^{(\pm)}_{\rm asy}(\nu, t)+\frac{1}{\pi}\int_0^{\nu_M} dx\,\mathrm{Im}B^{(+)}(x, t)\left(\frac{1}{x-\nu}\mp\frac{1}{x+\nu}\right)-\frac{b^{(\pm)}(t)}{\nu}\,S^{(\mp)}(\nu, t), \tag{1.15}$$

where

$$S^{(\pm)}(\nu, t)=\frac{1}{\pi}\int_0^{\nu_M} dx\,x^{\alpha(t)}\left(\frac{1}{x-\nu}\pm\frac{1}{x+\nu}\right). \tag{1.16}$$

Here $\nu_M=\nu_M(0)+t/4M$, and in our calculations we take $\nu_M(0)=1.85$ GeV. Finally, the large-ν limit of (1.14) and (1.15) yields the FESR which the amplitudes must satisfy.[9] In the present work we use the lowest-moment FESR.

III. DETAILS OF THE PROCEDURE

From the formalism of Sec. II it is apparent that, given information on the imaginary parts of the amplitudes in both the low- and high-energy regions, we can calculate the complete amplitude through the dispersion relations (1.14) and (1.15).

The high-energy part is completely determined by the functions $a^{(\pm)}(t)$ and $b^{(\pm)}(t)$ of Eqs. (1.9). These we shall calculate on the basis of the amplitude analysis of Refs. 2 and 3 (BMI solution) by inverting the relations (1.3), (1.4). Our choice is motivated by the following features of this analysis:

(a) Concerning the vector exchange (K^*), the imaginary parts of both the flip ($\mathrm{Im}F_1^{(-)}$) and nonflip ($\mathrm{Im}F_0^{(-)}$) SHA have the t structure of the dual absorptive model (DAM),[10,11] i.e., of Bessel-function form $\sim J_n(R\sqrt{-t})$, with $R\approx 1$ fermi. It is well known that such a structure for the vector exchange (ρ) is supported by several amplitude analyses of $\pi^-p\to\pi^0 n$.[12]

(b) The imaginary parts of the flip amplitudes for vector and tensor (K^{**}) exchange are assumed to be exchange-degenerate (in our sign convention, $\mathrm{Im}\,F_1^{(+)}=-\mathrm{Im}F_1^{(-)}$). Analyses of KN charge-exchange reactions based on phenomenology[13] and FESR[14,8] as well as the t structure and relative magnitude of the $K^{\pm}p\to K^{\pm}p$ polarizations[14] indicate that this assumption is rather well satisfied by the corresponding vector (ρ) and tensor (A_2) exchanges. We consider this point a particularly attractive feature of the BMI solution.

(c) $\mathrm{Im}F_0^{(+)}(\nu, t)$ deviates somewhat from the t structure of DAM (it looks like a "displaced"

Bessel function of zeroth order). Such a deviation for the nonflip SHA of the tensor exchange has also been found in πN scattering analyses[15] and is consistent with the corresponding FESR.

(d) As a result of (a) and (c), EXD is broken for the imaginary parts of the nonflip amplitudes. The requirement of sizeable polarization for $\bar{K}N \to \pi\Lambda$ is easily seen to imply some amount of EXD breaking.

The low-energy integrals of Eqs. (1.14), (1.15) provide non-negligible corrections to the real parts at energies below 20 GeV. To calculate these we must resort to resonance saturation, since phase-shift analyses are not presently available. Unfortunately, there is a rather large unphysical region involved here, with $Y_1^*(1385)$, $N^*(1470)$, $N^*(1520)$, and $N^*(1535)$ all below threshold in hypercharge exchange, as well as the nucleon and Σ poles. Apart from the Born terms, the couplings of these resonances below threshold are not precisely known. In accord with Ref. 9, as a first approximation we take the unbroken SU(3) values of these couplings. The appropriate effective Lagrangians and the resonance contributions are given in Ref. 9 and will not be repeated here. In Table I we give the SU(3) values for the cou-

TABLE I. Resonance masses, spin parities, and coupling strengths for resonances above and below threshold for $K^-n \to \pi^-\Lambda$ (s channel) and $\pi^+n \to K^+\Lambda$ (u channel). The relative phase of the resonance contribution is given by ϕ_R in the convention of Ref. 9.

	$10^2(\Gamma_1\Gamma_2)^{1/2}$ (GeV)				
Name J^P	Exp. range [a]	Couplings of Ref. 9	Solution 1	Solution 2	ϕ_R
$\Sigma(1670)\frac{3}{2}^-$	0.2–0.75	0.5	0.676	0.676	−1
$\Sigma(1750)\frac{1}{2}^-$	0.7–2.5	2.0	2.29	2.29	+1
$\Sigma(1765)\frac{5}{2}^-$	1.5–4.8	2.72	7.50	7.50	+1
$\Sigma(1915)\frac{5}{2}^+$	0.35–1.5	0.49	1.51	1.51	+1
$\Sigma(1920)\frac{1}{2}^+$ [b]	1.3–3.8	2.38	3.6	3.6	+1
$\Sigma(1940)\frac{3}{2}^-$	1.2–5.5	3.92	2.64	2.64	+1
$\Sigma(2030)\frac{7}{2}^+$	1.15–3.2	3.4	0.775	0.775	−1
$\Sigma(2080)\frac{3}{2}^+$	0.64–3.5	2.25	2.49	2.49	+1
$N(1675)\frac{5}{2}^-$	<0.5	0.18	0.0	−0.392	−1
$N(1688)\frac{5}{2}^+$	<0.5	0.10	0.0	0.0	−1
$N(1700)\frac{1}{2}^-$	1.8–4.2	3.4	2.02	2.02	−1
$N(1780)\frac{1}{2}^+$	0.5–4.3	1.1	0.5	0.5	+1
$N(1860)\frac{3}{2}^+$	1.0–3.7	1.48	0.7	0.7	−1
			Couplings of resonances below threshold		
			$G(\Sigma^*\pi^-\Lambda)G(\Sigma^*K^-n)$		
$\Sigma(1385)\frac{3}{2}^+$	−7.5– −1.86 [d]	−4.64 [e]	−7.44	−7.44	
			$G(N^*\pi^+N)G(N^*K^+\Lambda)$		
$N(1470)\frac{1}{2}^+$	−43.8– −14.6 [c]	−29.2 [e]	−28.7	−28.7	
$N(1518)\frac{3}{2}^-$	0.056–0.17 [c]	0.113 [e]	0.119	0.119	
$N(1550)\frac{1}{2}^-$	−18.3– −6.1 [c]	−12.2 [e]	−8.37	−8.37	

[a] Reference 16.
[b] Listed as $\Sigma(1880)$ in Ref. 16 (Data Card Listings, average mass ≃1920 MeV).
[c] Determined by ±50% of value of column 3.
[d] Determined by ±60% of value of column 3.
[e] Corresponding to F/D ratio of Ref. 9 (Table IV).

plings of the resonances below threshold, as well as the experimental range of values for the product $(\Gamma_1\Gamma_2)^{1/2}$ of the partial widths Γ_1 and Γ_2 for the decay of resonances above threshold into the $\pi\Lambda$ and $\bar{K}N$ channels.[16] The set of resonances presented in Table I is the same as in Ref. 9; this contains all the established Σ resonances (up to the mass of interest, $M_R = 2.08$ GeV) as well as some Σ resonances whose existence is very likely.[16]

The partial-wave decompositions of the A and B amplitudes are well known.[9] The contributions of the resonances above threshold to both the FESR and the dispersion integrals of Eqs. (1.14), (1.15) will be calculated in the narrow-resonance approximation, where

$$\mathrm{Im}F_{l\pm} = \frac{\pi M_R \phi_R (\Gamma_1\Gamma_2)^{1/2}}{2M_N(p_R p_R')^{1/2}}\,\delta(\nu-\nu_R)\,. \tag{2.1}$$

Here $f_{l\pm}$ is the partial-wave amplitude of parity $(-1)^{l+1}$, with $j = l\pm\frac{1}{2}$, Γ_i are the partial widths for decay of resonance R into $\bar{K}N$ and $\pi\Lambda$, ϕ_R is the relative phase of the resonance contribution (see Table I), and p_R (p_R') is the initial (final) c.m. momentum evaluated at $\sqrt{s} = M_R$ = resonance mass.

With the partial widths of the resonances chosen as in Ref. 9 and 10 (see Table I, third column) and with $a^{(\pm)}(t)$ and $b^{(\pm)}(t)$ calculated from the BMI solution of Fig. 2, the FESR for $A^{(+)}$ is badly violated [see Fig. 3(a), upper left graph].[17] The resulting $a^{(+)}(t)$ is of opposite sign to that of the BMI solution, thus completely breaking exchange degeneracy between $\mathrm{Im}F_1^{(+)}$ and $\mathrm{Im}F_1^{(-)}$ [feature (b) above]. The rest of the FESR are in fair agreement, at least for small $|t|$ [Fig. 3(a)].

There is, however, significant experimental uncertainty in some of the resonance elasticities and total widths; also, the couplings of the resonances below threshold are, in general, sensitive to the value of the F/D ratio.[9,16] Therefore, we have proceeded by allowing some variation in the resonance strengths. For the resonances above threshold we allow variations within the range of values of Table I (column 2), and in a few cases somewhat outside this range. For the resonances below threshold we allow variations in a range of about ±50% of the values of Ref. 9; for details see Table I. We allow no variations in the couplings of the nucleon and Σ poles.

In our final solutions (Fig. 3, Solutions 1, 2) all FESR are roughly accounted for, at least for $|t| \lesssim 0.7$ GeV^2. Also, the t structure of the BMI solution is fairly well reproduced (apart, perhaps, from $A^{(-)}$). For $|t| > 0.7$ GeV^2 we are unable to account for the FESR, at least for reasonable values of the resonance parameters.

The final values of our resonance parameters

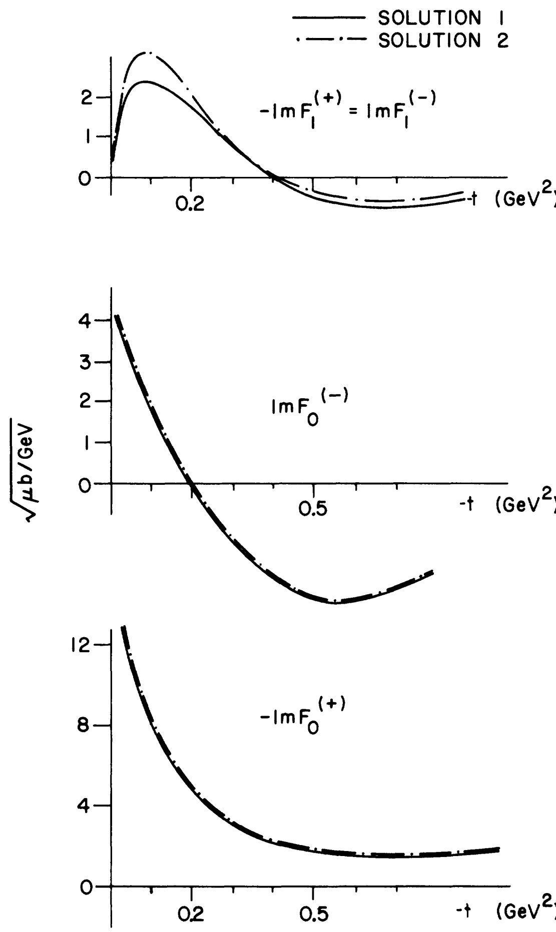

FIG. 2. Input imaginary parts of SHA. In our sign conventions exact EXD corresponds to $-\mathrm{Im}F_n^{(+)} = \mathrm{Im}F_n^{(-)}$, $n = 0, 1$ (Sec. II).

are given in Table I (fourth and fifth column). These same parameters are used to saturate $\mathrm{Im}A^{(\pm)}(\nu', t)$ and $\mathrm{Im}B^{(\pm)}(\nu', t)$ in the low-energy dispersion integrals of Eqs. (1.14), (1.15).

IV. RESULTS AND THEIR BASIC ASPECTS

We present in detail calculations with two different solutions:

(1) For Solution 1 the resonance parameters are given in the fourth column of Table I. The functions $a^{(\pm)}(t)$ and $b^{(\pm)}(t)$ have been calculated from the imaginary parts of the BMI solution of Fig. 2 (solid lines). Throughout Figs. 4–7 (see Refs. 18-29) the results of the calculations with this solution are shown with full lines.

(2) For Solution 2 the resonance parameters are given in the fifth column of Table I. In this solution we have allowed a change in sign of the $N(1675)$ contribution, still keeping its strength within experimental range. The functions $a^{(\pm)}(t)$

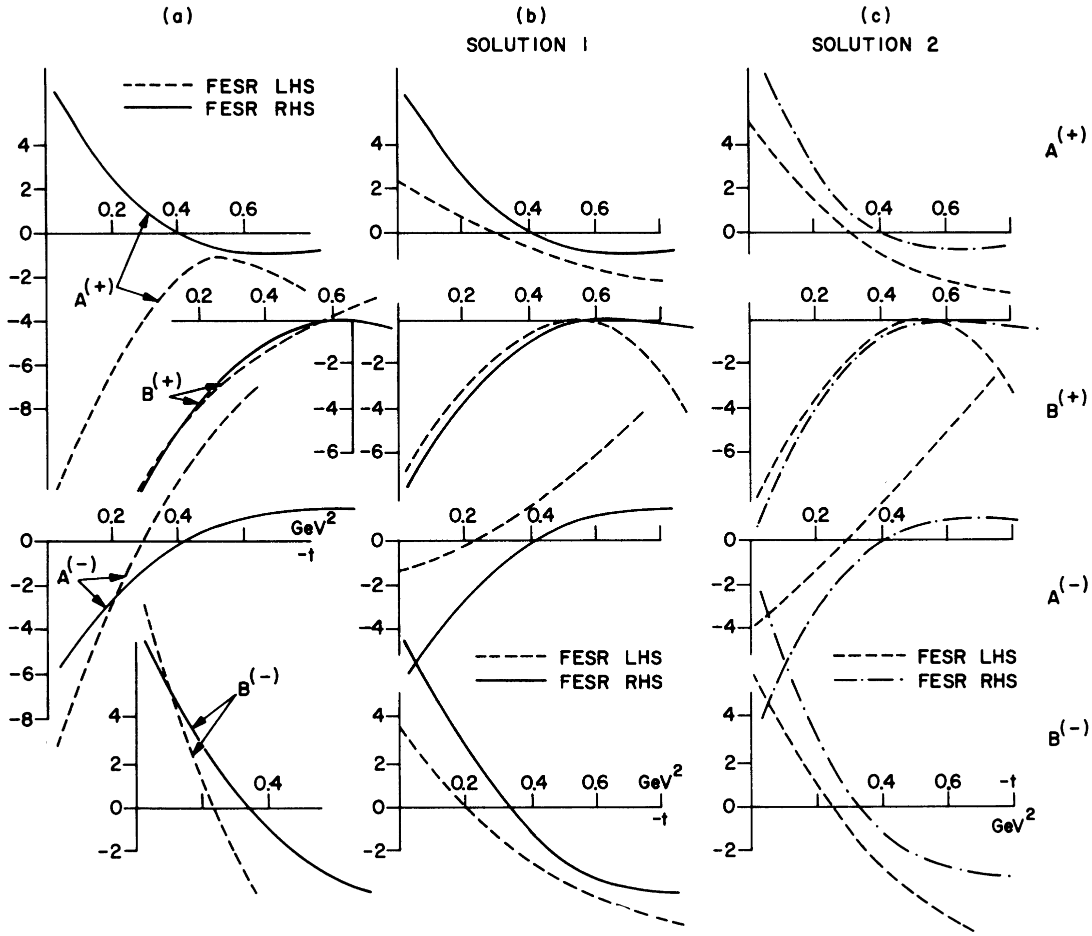

FIG. 3. LHS vs RHS of FESR for various cases: (a) LHS calculated from resonance couplings of Table I, column 3, vs RHS calculated from the imaginary parts of Solution 1 (≡ BMI solution, Fig. 2, solid lines); (b) LHS from Table I, column 4, vs RHS from the imaginary parts of Solution 1; and (c) LHS from Table I, column 5, vs RHS from the imaginary parts of Solution 2 (Fig. 2, dash-dotted lines).

and $b^{(\pm)}(t)$ have been calculated from the imaginary parts of Fig. 2 (dash-dotted lines); these differ from Solution 1 only in a small change of $\mathrm{Im}F_1^{(\pm)}$ (but always within the limits established by Barger *et al.*[2,3]). The main effect of these changes is in the polarization of $\pi^- p \to K^0\Lambda$ at $|t| \lesssim 0.15$ GeV^2; as we discuss below, this quantity is particularly sensitive on the exact input imaginary parts and resonance parameters. Also, the change in sign of the $N(1675)$ contribution somewhat improves the over-all agreement with FESR [Fig. 3(c)]. Throughout Figs. 4–7 the results of the calculations with this solution are shown with dash-dotted lines.

The resulting real parts of the SHA are qualitatively similar for the two solutions (Fig. 4) and their basic features can be summarized as follows.

(i) Flip amplitude of vector exchange ($\mathrm{Re}F_1^{(-)}$). This exhibits the characteristic "double-zero" structure. We understand this feature as follows. From Eqs. (1.4), (1.10), and (1.14) we obtain

$$[\mathrm{Re}F_1^{(-)}(\nu,t)]_{\mathrm{asy}} \equiv -\sqrt{-t}\,\mathrm{Re}A_{\mathrm{asy}}^{(-)}(\nu,t) = \tan\tfrac{1}{2}\pi\alpha\,\mathrm{Im}F_1^{(-)}(\nu,t). \qquad (4.1)$$

Since $\mathrm{Im}F_1^{(-)}(\nu,t)$ has a simple zero at $\alpha(t)=0$ ($t=-0.4$), $[\mathrm{Re}F_1^{(-)}]_{\mathrm{asy}}$ has a double zero. The complete $\mathrm{Re}F_1^{(-)} = -\sqrt{-t}\,\mathrm{Re}A^{(-)}$, as calculated from (1.14), contains also two extra terms. Expanding these extra terms in powers of $1/\nu$, we have

$$\frac{1}{\pi}\int_0^{\nu_M} dx\,\mathrm{Im}A^{(-)}(x,t)\left(\frac{1}{x-\nu}-\frac{1}{x+\nu}\right)-a^{(-)}(t)S^{(-)}(\nu,t) = -\frac{2}{\nu\pi}\left[\int_0^{\nu_M} dx\,\mathrm{Im}A^{(-)}(x,t) - \alpha^{(-)}(t)\,\frac{\nu_M^{\alpha(t)+1}}{\alpha(t)+1}\right]+O(1/\nu^3). \qquad (4.2)$$

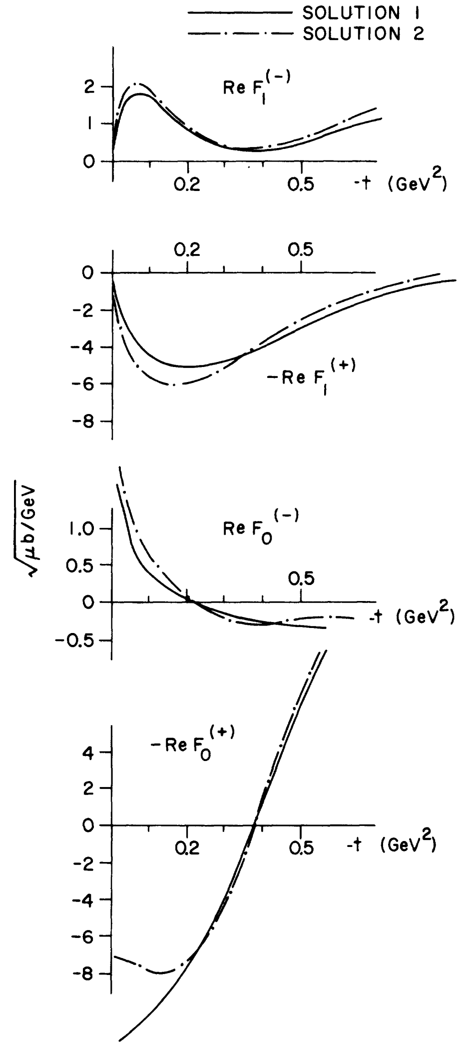

FIG. 4. Calculated real parts of SHA.

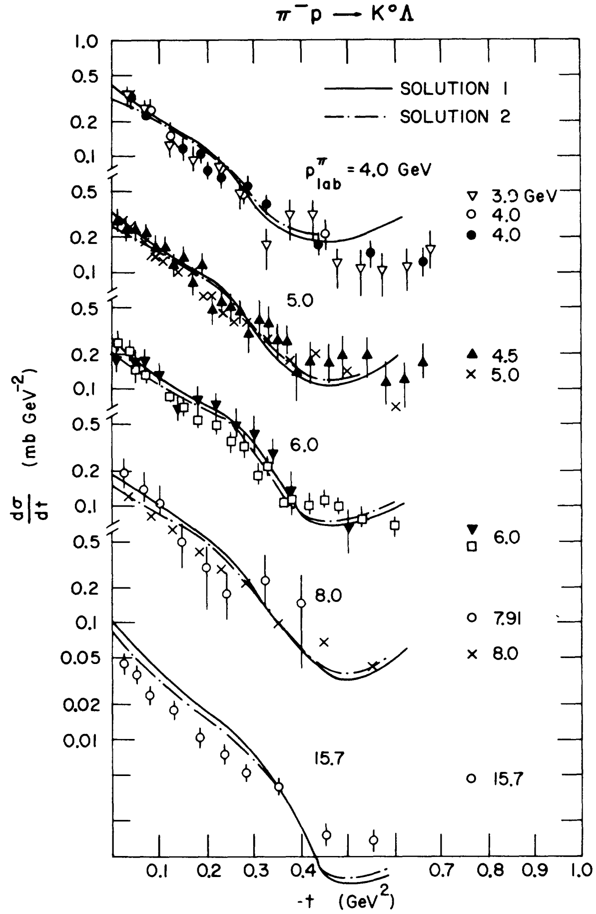

FIG. 5. Calculated differential cross sections for $\pi^- p \to K^0\Lambda$ data: ▽ 3.9 GeV, Ref. 18; ○ 4.0 GeV, Ref. 19; ● 4.0, ×5.0, and □ 6.0 GeV, Ref. 20; ▲ 4.5 and ▼ 6.0 GeV, Ref. 21; ○ 7.91 GeV, Ref. 22; × 8.0 and ○ 15.7 GeV, Ref. 23.

The quantity in square brackets is precisely the difference between the left-hand side (LHS) and the right-hand side (RHS) of the zero-moment FESR for $A^{(-)}$.[9] Since this FESR is somehow satisfied, the quantity in brackets is relatively small and, being also divided by ν, implies a relatively small correction to $\mathrm{Re}A^{(-)}_{\mathrm{asy}}$ at high energy. The rest of the terms in the expansion of Eq. (4.2) are proportional to the differences of higher-moment FESR for $A^{(-)}$ and provide also small corrections at large ν.

It should be stressed, however, that the correction to $\mathrm{Re}A^{(-)}_{\mathrm{asy}}$, implied by the extra terms of (4.2), and the similar corrections to $\mathrm{Re}A^{(+)}_{\mathrm{asy}}$ and $\mathrm{Re}B^{(\pm)}_{\mathrm{asy}}$ are very important in our approach. This particularly holds for the nonflip amplitudes (see below), where these corrections are sizable and significantly affect the magnitude of sensitive quantities, such as polarizations. E.g., if in our calculations [with $\alpha_\pm' = \alpha_\pm = \alpha(t)$] we were to use $\mathrm{Re}A^{(\pm)} = \mathrm{Re}A^{(\pm)}_{\mathrm{asy}}$ and $\mathrm{Re}B^{(\pm)} = \mathrm{Re}B^{(+)}_{\mathrm{asy}}$, we would get zero polarizations for both $\pi N \to K\Lambda$ and $\bar{K}N \to \pi\Lambda$. We believe that our procedure gives reasonably accurate corrections because, as we mentioned in Sec. II, the expressions (1.9) [or equivalent expressions of the form $\mathrm{Im}F^{(\pm)}_n = b^{(\pm)}_n(t)\nu^{\alpha(t)}$ (Refs. 6–8)] have been found to parametrize correctly the imaginary parts of the amplitudes above $p_{\mathrm{lab}} \approx 3$ GeV (Refs 4–9); once these forms are accepted as correct high-energy parametrizations of the imaginary parts, analyticity should, through DR, give the best real parts.

Equation (4.2) shows that the magnitude of these corrections depends on the difference between LHS and RHS of FESR. The point here is that, in general, the expressions (1.9), although good parametrizations at high energy, can only approximately satisfy FESR[4,8,9] (in particular for several moments), because FESR involve extrapolations of (1.9) down to threshold. To improve the agreement with FESR we must replace (1.9) by more sophisticated forms, like

$$\mathrm{Im}B^{(\pm)} = b^{(\pm)}(t)\nu^{\alpha(t)-1} + \bar{b}^{(t)}(t)\nu^{\bar{\alpha}(t)-1}$$

[with $\bar{\alpha}(t) < \alpha(t)$]. However, then the extra term $\bar{b}^{(t)}\nu^{\bar{\alpha}-1}$ provides an equivalent correction to $\mathrm{Re}B^{(\pm)}$ (see Appendix of Ref. 8 for detailed discussion).

(ii) Flip amplitude of tensor exchange ($\mathrm{Re}F_1^{(+)}$). This is smooth and rather strong near $t = -0.4$ (no double zero). An argument similar to that of (4.2) shows that its over-all structure should be close to the form

$$[\mathrm{Re}F_1^{(+)}(\nu, t)]_{\mathrm{asy}} = -\sqrt{-t}\,\mathrm{Re}A_{\mathrm{asy}}^{(+)}(\nu, t)$$
$$= -\cot\tfrac{1}{2}\pi\alpha\,\mathrm{Im}F_1^{(+)}(\nu, t)\,. \qquad (4.3)$$

$\mathrm{Im}F_1^{(+)}$ has a zero at $t = -0.4$, but it is canceled by $\cot\frac{1}{2}\pi\alpha$.

We may conclude that both $F_1^{(-)}$ and $F_1^{(+)}$ of our solutions are, roughly, dominated by a single Regge pole (with small absorption or other corrections).

(iii) Nonflip amplitudes ($\mathrm{Re}F_0^{(\pm)}$). Our solutions for $\mathrm{Re}F_0^{(-)}$ (Fig. 4) are in agreement with those of Barger *et al.* (within the limits set by their analysis[3]). In particular our Solution 1 (solid line of Fig. 4) gives also $\mathrm{Re}F_0^{(+)}$ in agreement with Refs. 2 and 3. Notice the change of sign near $t = -0.4$ of both our solutions for $\mathrm{Re}F_0^{(+)}$; this seems to be a common conclusion of several analyses concerning the real part of the nonflip amplitude for tensor exchange.[2,3,30,31] As we have seen (Fig. 3),

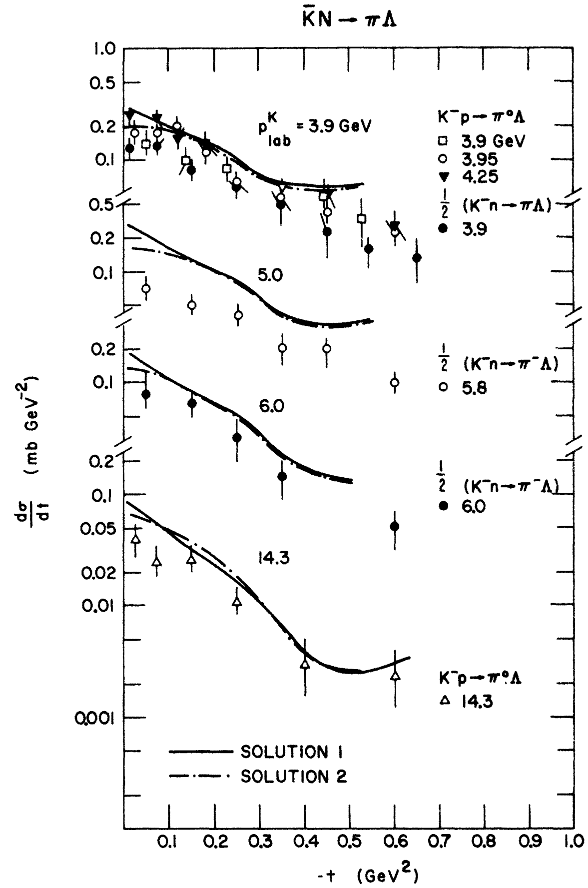

FIG. 6. Calculated differential cross sections for $\bar{K}N \to \pi\Lambda_-$ data: □ 3.9 GeV, Ref. 24; ○ 3.95 GeV, Ref. 25; ▼ 4.25 GeV, Ref. 26; ● 3.9 GeV, Ref. 27; ○ 5.8 and ● 6.0 GeV, Ref. 28; △ 14.3 GeV, Ref. 29.

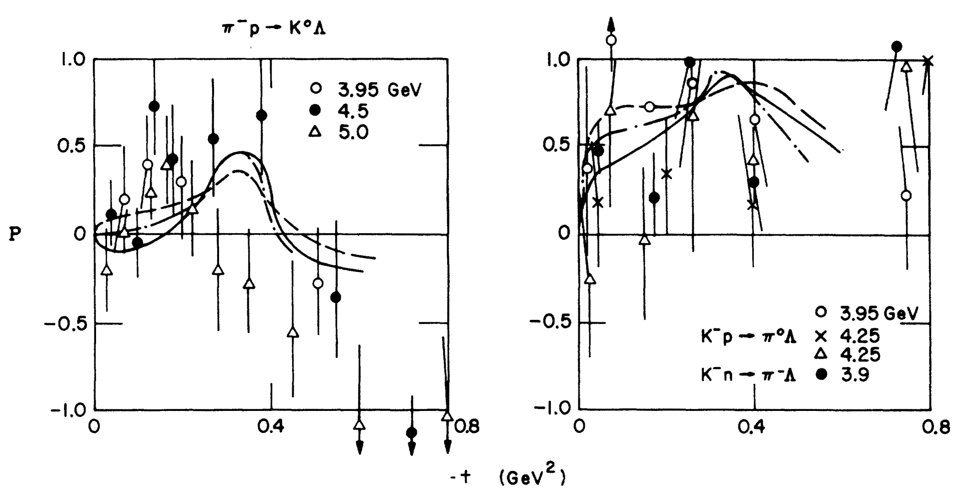

FIG. 7. Polarization at 4 GeV for $\pi^-p \to K^0\Lambda$ and $\bar{K}N \to \pi\Lambda_-$. Full lines: Solution 1. Dash-dotted lines: Solution 2. Dashed lines: Solution 1 with only $|\mathrm{Im}F_1^{(\pm)}|$ increased by 30%. Data for $\pi^-p \to K^0\Lambda$: ○ 3.95 GeV, Ref. 18; △ 5.0 GeV, Ref. 20; ● 4.5 GeV, Ref. 21. Data for $\bar{K}N \to \pi\Lambda$: ○ 3.95 GeV, Ref. 25; × 4.25 GeV, Ref. 24; △ 4.25 GeV, Ref. 26; ● 3.9 GeV, Ref. 27.

for large $|t|$ our FESR are badly violated; this results in a $\mathrm{Re}F_0^{(+)}$ somewhat too large.

A single Regge-pole exchange [with a nonsense wrong-signature factor $\alpha(t)$ in the residue of $F_0^{(-)}$ and a ghost-eliminating factor $\alpha(t)$ in the residue of $F_0^{(+)}$] would produce $\mathrm{Im}\,F_0^{(\pm)}$ and $\mathrm{Re}\,F_0^{(\pm)}$ completely different from those of our solutions (and of Refs. 2 and 3). Clearly, our nonflip amplitudes require large corrections to the single Regge-pole exchange.

With our solutions we now proceed in the calculation of the differential cross sections for $\pi N\rightarrow K\Lambda$ and $\bar{K}N\rightarrow\pi\Lambda$ at several energies (Figs. 5 and 6). Our results, although not comparable with fits of high quality, for $0< -t \lesssim 0.6$ are in fair agreement with, and exhibit the basic features of, the experimental data. In general $d\sigma/dt(\pi N\rightarrow K\Lambda)$ is steeper than $d\sigma/dt(\bar{K}N\rightarrow\pi\Lambda)$ (Refs. 1, 9), and for $|t|\gtrsim 0.15$ GeV^2 we have $d\sigma/dt(\bar{K}N\rightarrow\pi\Lambda) > d\sigma/dt(\pi N\rightarrow K\Lambda)$. It is well known that absorptive Regge-cut models fail completely to account for this fact.[32] With the common trajectory $\alpha(t)$ of Eq. (1.13) the energy variation of the cross sections is also fairly well accounted for. Clearly, improvements are possible, e.g., by choosing somewhat different effective Regge exponents in Eqs. (1.12) [i.e., $\alpha'_\pm(t)\neq\alpha_\pm(t)$]. Again, as a result of breaking FESR, for $|t|\gtrsim 0.6$ we obtain cross sections which are too large.

Finally, Fig. 7 presents our calculated polarizations at 4 GeV. For $\bar{K}N\rightarrow\pi\Lambda$ we find large positive polarization, in accord with all experiments. For $\pi N\rightarrow K\Lambda$ the experimental situation is less clear; our solutions are in accord with the data of Crennell *et al.*[21] In general, our polarizations are positive near $t=-0.3$ and change sign near $t=-0.4$. However, for small $|t|$ ($\lesssim 0.2$) our $\pi N\rightarrow K\Lambda$ polarizations are very sensitive to the input imaginary parts of SHA and to the exact values of the resonance strengths. To illustrate this we have increased by 30% the magnitude of $\mathrm{Im}F_1^{(\pm)}$ of Solution 1, keeping the t dependence, as well as the resonance strengths and $\mathrm{Im}F_0^{(\pm)}$, the same. The corresponding polarizations are shown in Fig. 7 (dashed lines). Compared with Solution 1 (solid lines), the $\pi N\rightarrow K\Lambda$ polarization changes sign for $|t|\lesssim 0.2$ GeV^2. In contrast, the differential cross sections do not change appreciably.

Finally we note that both Solutions 1 and 2 lead to helicity correlation parameters $T[\sim\mathrm{Re}(F_0F_1^*)]$ of the same magnitude and t structure of Refs. 2 and 3.[33]

V. CONCLUSIONS

With the BMI solution for the imaginary parts as a point of departure we have produced an amplitude analysis that has the properties (*a*)–(*c*) listed in the Introduction.

A basic feature of our solutions is that the imaginary parts of the flip amplitudes for vector and tensor exchange satisfy EXD [in our sign convention: $\mathrm{Im}F_1^{(-)}(\nu,t)=-\mathrm{Im}F_1^{(+)}(\nu,t)$ for $\nu>\nu_M$]; however EXD is broken for the imaginary parts of the nonflip amplitudes [$\mathrm{Im}F_0^{(+)}\approx -3\,\mathrm{Im}F_0^{(-)}$ near $t=0$]. On the other hand, we have seen (Sec. IV) that our solutions for $F_1^{(\pm)}$ are approximately consistent with dominance of a single Regge-pole exchange; in contrast, our solutions for $F_0^{(\pm)}$ must involve strong corrections to the leading Regge poles.

It is then possible that the leading Regge poles satisfy EXD to a good approximation, but for the corrections, EXD is significantly broken. In hypercharge-exchange reactions the nonflip amplitudes are particularly strong; this is probably why, at least for energies $\lesssim 15$ GeV, EXD is broken.[1,34]

If the corrections to the leading Regge poles come from lower-lying singularities in complex angular momentum, we expect that, as the energy increases, EXD will improve in hypercharge-exchange reactions. If, however, the corrections come from singularities with trajectories comparable to those of the leading poles, EXD will still be broken at higher energy.

ACKNOWLEDGMENTS

One of us (A. P. C.) would like to thank Dr. Kwan-Wu Lai and Dr. N. P. Samios for several helpful discussions and for the hospitality extended to him at Brookhaven. We would also like to thank Dr. V. D. Barger and Dr. M. Scadron for useful discussions.

---

*Research supported by Department of Physics, State University College of Arts and Science, Plattsburgh, New York.

†Permanent address: Department of Physics, McGill University, Montreal, Quebec, Canada.

‡Work supported in part by the U. S. Atomic Energy Commission.

§Work also supported by the National Research Council of Canada.

[1] Kwan-Wu Lai and J. Louie, Nucl. Phys. B19, 205 (1970).

[2] V. D. Barger and A. D. Martin, Phys. Lett. 39B, 379 (1972).

[3] A. C. Irving, A. D. Martin, and V. D. Barger, Nuovo Cimento 16A, 573 (1973).

[4]G. Ghandour and R. G. Moorhouse, Phys. Rev. D 6, 856 (1972).

[5]M. Coirier, J. Guillaume, Y. Leroyer, and Ph. Salin, Nucl. Phys. B44, 157 (1972).

[6]E. N. Argyres and A. P. Contogouris, Phys. Rev. D 6, 2018 (1972); E. N. Argyres, A. P. Contogouris, and M. Svec, *ibid.* 8, 184 (1973).

[7]M. Hontebeyrie, J. Procureur, and Ph. Salin, Nucl. Phys. B55, 83 (1973); I. Barbour and R. G. Moorhouse, CERN Report No. TH-1712, 1973 (unpublished).

[8]E. N. Argyres, A. P. Contogouris, J. P. Holden, and M. Svec, Phys. Rev. D 8, 2068 (1973); this paper also discusses certain theoretical aspects of the over-all. approach. Application of the same method to KN charge-exchange reactions is under completion.

[9]R. D. Field, Jr., and J. D. Jackson, Phys. Rev. D 4, 693 (1971); R. D. Field, Jr., Ph.D. thesis, LBL Report No. LBL-33, 1971 (unpublished).

[10]H. Harari, Phys. Rev. Lett. 26, 1400 (1971).

[11]M. Davier and H. Harari, Phys. Lett. 35B, 239 (1971).

[12]F. Halzen and C.Michael, Phys. Lett. 36B, 367 (1971); R. L. Kelly, *ibid.* 39B, 635 (1971); G. Cozzika *et al.*, *ibid.* 40B, 281 (1972); M. Giffon, Nuovo Cimento 7A, 705 (1972); P. Johnson *et al.*, Phys. Rev. Lett. 30, 242 (1973); Y. Kohsaka and F. Takagi, Tohoku Univ. Report No. TU/73/104 (unpublished).

[13]V. D. Barger and D. B. Cline, *Phenomenological Theories of High Energy Scattering* (Benjamin, New York, 1968).

[14]G. V. Dass and C. Michael, Phys. Rev. 175, 1774 (1968); L. Dick, in *Proceedings of the Second International Conference on Polarized Targets*, edited by G. Shapiro (Univ. of California Press, Berkeley, California, 1971), p. 167.

[15]V. D. Barger, K. Geer, and F. Halzen, Nucl. Phys. B49, 302 (1972).

[16]Particle Data Group, LBL Report No. LBL-100, 1972 (unpublished); Rev. Mod. Phys. 42, 87 (1970); N. P. Samios, M. Goldberg, and B. T. Meadows, BNL Report No. BNL 17851, 1973 (unpublished).

[17]In Ref. 9 it is stressed that, with their choice of resonance strengths, EXD between $A'^{(+)}$ and $A'^{(-)}$ is violated (for the definition of $A'^{(\pm)}$, see Ref. 9).

[18]M. Abramovich *et al.*, Nucl. Phys. B27, 477 (1971).

[19]O. I. Dahl *et al.*, Phys. Rev. 163, 1430 (1967).

[20]C. E. W. Ward *et al.*, contribution to the XVI International Conference on High Energy Physics, Chicago-Batavia, Ill., 1972 (unpublished).

[21]D. J. Crennell *et al.*, Phys. Rev. D 6, 1220 (1972).

[22]R. Ehrlich *et al.*, Phys. Rev. 152, 1194 (1966).

[23]E. H. Willen *et al.*, BNL Report No. BNL 16681, 1972 (unpublished).

[24]M.Aguilar-Benitez *et al.*, Phys. Rev. D 6, 29 (1972).

[25]L. Moscosco *et al.*, Nucl. Phys. B36, 332 (1972).

[26]R. Blokzigl *et al.*, Nucl. Phys. B51, 535 (1973).

[27]D. J. Crennell *et al.*, Phys. Rev. Lett. 23, 1347 (1969).

[28]W. Fickinger *et al.*, in *Phenomenology in Particle Physics, 1971*, proceedings of the conference held at Caltech, 1971, edited by C. B. Chiu, G. C. Fox, and A. J. G. Hey (Caltech, Pasadena, 1971), p. 469.

[29]R. J. Miller *et al.*, contribution to the XVI International Conference on High Energy Physics, Chicago-Batavia, Ill., 1972 (unpublished).

[30]C. B. Chiu and E. Ugaz, Phys. Lett. 43B, 327 (1973).

[31]J. S. Loos and J. A. J. Matthews, Phys. Rev. D 6, 2463 (1972). This work also presents a complete amplitude analysis of $\pi N \to K\Lambda(\Sigma)$ and $\bar{K}N \to \pi\Lambda(\Sigma)$. Although this analysis has certain features in common with Refs. 2 and 3, EXD of the K^*-K^{**} imaginary parts is broken by factors ranging from 5 (for Λ-production reactions) to 8 (for Σ production), and in fact for both the nonflip and the flip SHAs. We find this feature rather unattractive. Some criticism of this analysis with respect to its implications for $K^-p \to \eta\Lambda$ and $K^-p \to \eta'\Lambda$ has also been advanced (see Ref. 3).

[32]See, e.g., A. D. Martin, in *Proceedings of the Seventh Rencontre de Moriond*, edited by J. Tran Thanh Van (CNRS, Paris, 1972).

[33]A decisive test of the BMI solution (Refs. 2, 3) (or ours) versus that of Ref. 32 can be made by measuring the decay correlation parameters T in particular for $\pi N \to K\Lambda$, $\pi N \to K\Sigma$, and $\bar{K}N \to \pi\Sigma$. In all cases the BMI solution gives smooth and large $|T|$ with no change of sign in the whole range $0 < -t \lesssim 1$ GeV^2 (see Refs. 2 and 3). In contrast, T of Ref. 32 varies rapidly, changing sign at $-t \approx 0.2$ GeV^2 and at $-t \gtrsim 0.6$ GeV^2.

[34]A. Bashian *et al.*, Phys. Rev. D 4, 2667 (1972). Experiment shows that for $-t \gtrsim 0.4$ GeV^2 the $\pi^+p \to K^+\Sigma^+$ polarization is appreciable even at $p_{lab} = 14$ GeV.